Am J Physiol Regul Integr Comp Physiol 294: R311–R320, 2008.
First published November 21, 2007; doi:10.1152/ajpregu.00735.2007.

Attenuation of acute and chronic liver injury in rats by iron-deficient diet

Kohji Otogawa,[1]* Tomohiro Ogawa,[1]* Ryoko Shiga,[2] Kazuki Nakatani,[2] Kazuo Ikeda,[2] Yuji Nakajima,[2] and Norifumi Kawada[1]

Departments of [1]Hepatology and [2]Anatomy, Graduate School of Medicine, Osaka City University, Osaka, Japan

Submitted 9 October 2007; accepted in final form 15 November 2007

Otogawa K, Ogawa T, Shiga R, Nakatani K, Ikeda K, Nakajima Y, Kawada N. Attenuation of acute and chronic liver injury in rats by iron-deficient diet. *Am J Physiol Regul Integr Comp Physiol* 294: R311–R320, 2008. First published November 21, 2007; doi:10.1152/ajpregu.00735.2007.—Oxidative stress due to iron deposition in hepatocytes or Kupffer cells contributes to the initiation and perpetuation of liver injury. The aim of this study was to clarify the association between dietary iron and liver injuries in rats. Liver injury was initiated by the administration of thioacetamide or ligation of the common bile duct in rats fed a control diet (CD) or iron-deficient diet (ID). In the acute liver injury model induced by thioacetamide, serum levels of aspartate aminotransferase and alanine aminotransferase, as well as hepatic levels of lipid peroxide and 4-hydroxynonenal, were significantly decreased in the ID group. The expression of 8-hydroxydeoxyguanosine and terminal deoxynucleotidyl transferase biotin-dUTP nick-end labeling positivity showed a similar tendency. The expression of interleukin-1β and monocyte chemotactic protein-1 mRNA was suppressed in the ID group. In liver fibrosis induced by an 8-wk thioacetamide administration, ID suppressed collagen deposition and smooth muscle α-actin expression. The expressions of collagen 1A2, transforming growth factor β, and platelet-derived growth factor receptor β mRNA were all significantly decreased in the ID group. Liver fibrosis was additionally suppressed in the bile-duct ligation model by ID. In culture experiments, deferoxamine attenuated the activation process of rat hepatic stellate cells, a dominant producer of collagen in the liver. In conclusion, reduced dietary iron is considered to be beneficial in improving acute and chronic liver injuries by reducing oxidative stress. The results obtained in this study support the clinical usefulness of an iron-reduced diet for the improvement of liver disorders induced by chronic hepatitis C and alcoholic/nonalcoholic steatohepatitis.

oxidative stress; fibrosis; stellate cell; Kupffer cell

IN GENERAL, THE METABOLISM, uptake, and excretion of iron in the body are strictly regulated (1, 7, 33). The majority of iron in the body is contained in erythrocytes as a component of hemoglobin and circulates throughout the whole body to allow vital biological processes. Most of the other iron is stored in the spleen and liver as a component of iron-containing enzymes such as cytochrome *P*-450. However, the presence of free iron and deposition of iron in cells often occurs under some pathological conditions, triggering oxidative stress and inflammation (4, 24, 30). For instance, hemochromatosis and iron-overload due to the excessive intake of iron-containing medicine and supplements frequently induce liver cell damage and, in some cases, cirrhosis (2, 31).

It has been shown that the deposition of iron occurs frequently in some liver diseases, including viral hepatitis (3, 6), alcoholic liver injury (5, 38), and nonalcoholic steatohepatitis (NASH) (8, 36). Iron reduction by phlebotomy reduced mean serum alanine transaminase (ALT) activity and induced disappearance of iron deposits in the liver in chronic active hepatitis C patients (9, 13). Thus, iron is considered to play a role in the onset of liver cell damage. Free iron induces the production of proinflammatory and fibrogenic mediators such as TNF-α and transforming growth factor β (TGF-β) and nuclear factor-κB (NF-κB) activation in hepatic macrophages (17, 35, 39). Recently, we showed that the phagocytosis of erythrocytes by hepatic macrophages results in the deposition of iron derived from hemoglobin in the liver and contributes to the pathogenesis of NASH in a rabbit model (29). In that study, we clearly showed that iron reduction by phlebotomy lowers iron deposition in the liver and spleen and attenuates the progression of liver fibrosis.

Free metal ions are known to be important for the production of free radicals, among which iron is most potent in vivo (24, 30). The generated free radicals induce lipid peroxidation, DNA breakage, and 8-hydroxy-2′-deoxyguanosine (8-OHdG) formation, resulting in tissue damage and DNA mutagenesis (11, 18, 37). Although it has been clarified that iron overload may be associated with hepatitis, cirrhosis, or liver cancer, it is still unclear whether an iron-restricted diet has protective effects against acute liver injury and fibrosis. We have postulated that hepatic iron depletion contributes to the attenuation of liver injury caused in rats by the administration of the hepatotoxin thioacetamide (TAA).

Herein, we showed that iron depletion has the potential to attenuate acute liver damage and fibrosis in rats induced by TAA and ligation of the common bile duct. Analysis of this mechanism revealed that iron depletion hampers oxidative stress, inflammation, and hepatic stellate cell activation, resulting in the inhibition of liver fibrosis.

MATERIALS AND METHODS

Animals. Pathogen-free male Wistar rats were obtained from SLC (Shizuoka, Japan). Animals were housed at a constant temperature and supplied with laboratory chow and water ad libitum. The experimental protocol was approved by the Animal Research Committee of Osaka City University (Guide for Animal Experiments, Osaka City University).

Animal models. Rats weighing 200 to 230 g were fed a control diet (CD; $n = 5$) or an iron-deficient diet (ID; $n = 5$; Oriental Yeast, Tokyo, Japan) for 4 wk. The contents of the CD and ID are shown in Table 1. Successively, the rats were intraperitoneally administered TAA (100 mg/body wt; Wako, Osaka, Japan) to produce an acute liver failure model. Rats were killed to excise the liver at 48 h after TAA administration. Alternatively, the survival of rats with acute

* Kohji Otogawa and Tomohiro Ogawa contributed equally to this study.

Address for reprint requests and other correspondence: N. Kawada, Dept. of Hepatology, Graduate School of Medicine, Osaka City Univ., 1-4-3, Asahimachi, Abeno, Osaka 545-8585, Japan (e-mail: kawadanori @med.osaka-cu.ac.jp).

The costs of publication of this article were defrayed in part by the payment of page charges. The article must therefore be hereby marked "*advertisement*" in accordance with 18 U.S.C. Section 1734 solely to indicate this fact.

Table 1. *Nutrition contents of control and iron-deficient diets*

Nutrition Contents	Control Diet	Iron-Deficient Diet
Total fat, %	6.4	6.4
Soy protein, %	27.5	27.5
Total carbohydrates, %	46.6	46.6
Salt mixture, %	8.1	8.1
Iron, mg/100 g	12.3	0.03
Fiber, %	4.1	4.1
Moisture, %	6.9	6.9

The other contents, including copper and vitamins, were equilibrated.

liver failure induced by TAA administration (60 mg/body wt) was observed in CD ($n = 15$) and ID ($n = 15$) groups until 4 days.

As a liver fibrosis model, rats were supplied with CD ($n = 5$) or ID ($n = 5$) for 4 wk and successively intraperitoneally administrated with TAA (50 mg/body wt) twice a week for 6 wk (26).

Preparation of hepatic stellate cells. Hepatic stellate cells were isolated from male Wistar rats, as previously described (20). Isolated stellate cells were cultured on plastic dishes in DMEM containing 10% FCS and antibiotics (DMEM/FCS). On *day 2* of primary culture, the medium was replaced by DMEM/FCS with or without test agents, and the culture was continued for another 3 days. Then, the cells were prepared for morphological observation, immunoblotting, immunostaining, and a thymidine-incorporation assay.

Determination of serum concentrations of iron, aspartate aminotransferase, alanine aminotransferase, and lipid peroxide. Blood was collected from the inferior vena cava and centrifuged at 3,000 rpm for 10 min at room temperature. Serum concentrations of iron, aspartate aminotransferase (AST), ALT, and lipid peroxide (LPO) were measured at Special Reference Laboratories (SRL; Osaka, Japan).

Determination of hepatic iron and LPO. The liver of each animal was perfused via the portal vein with PBS to remove the blood. The hepatic free iron concentration and LPO were measured at SRL. The free iron concentration in the liver was measured by Nitroso-PSAP method.

Histochemical and immunohistochemical staining. The liver of each animal was perfused through the portal vein with PBS to remove the blood and then fixed with 4% paraformaldehyde or Bouin's fluid. The liver tissues were embedded, cut into 5-μm-thick sections, and then underwent hematoxylin and eosin and Sirius red staining, as described previously (19). Immunostaining using monoclonal antibodies against 8-OHdG (Japan Institute for the Control of Aging (JaICA), Shizuoka, Japan) and smooth muscle α-actin (αSMA; Sigma Chemical, St. Louis, MO) was performed according to the methods described previously (29).

Terminal deoxynucleotidyl transferase-mediated deoxyuridine triphosphate nick-end labeling staining. For the detection of apoptosis, paraffin sections were stained by the terminal deoxynucleotidyl transferase-mediated deoxyuridine triphosphate nick-end labeling (TUNEL) technique using an in situ apoptosis detection kit (Takara, Shiga, Japan), according to the manufacturer's instructions.

Determination of caspase-3 and -8 activities. Caspase-3 and -8 activities were determined using the caspase-3 and -8 colorimetric assay kits (Biovision, Mountain View, CA), respectively, as previously described (25) according to the manufacturer's recommendation.

Immunoblotting. Protein samples (10 μg) were subjected to SDS-PAGE, and then transferred onto Immobilon P membranes (Millipore, Bedford, MA) (22). After blocking, the membranes were treated with primary antibodies against 4-hydroxy-2-nonenal (4-HNE; JaICA), platelet-derived growth factor receptor β (PDGFRβ, Santa Cruz Biotechnology, Santa Cruz, CA), αSMA, ERK1/2 (Cell Signaling Technology, Beverly, MA), phospho-ERK1/2 (Thr^{202}/Tyr^{204}) (Cell Signaling Technology), Akt (Cell Signaling Technology), and phospho-Akt (Ser^{473}) (Cell Signaling Technology), and then were incubated with peroxidase-conjugated secondary antibodies. Immunoreactive bands were visualized using the enhanced chemiluminescence system (Amersham Pharmacia Biotech, Little Chalfont, Buckinghamshire, UK) and with an LAS 1000 (Fuji Photo Film, Kanagawa, Japan). The density of bands was analyzed using a Bio-Rad GS-700 densitometer (Bio-Rad, Hercules, CA).

Real-time RT-PCR. Total RNAs for the RT-PCR were extracted from the livers using the RNeasy total RNA system (Qiagen, Hilden, Germany). cDNAs were synthesized using 1 μg of total RNA, ReverTra Ace (Toyobo, Osaka, Japan), and $Oligo(dT)_{12–18}$ primer according to the manufacturer's instructions. The expression levels of genes were measured by real-time RT-PCR using the cDNAs, real-time PCR master mix (Toyobo), and a set of gene-specific oligonucleotide primers and the TaqMan probe listed in Table 2.

[^{3}H]Thymidine-incorporation assay. Isolated stellate cells were cultured on plastic dishes for 2 days in DMEM/FCS. The medium was then replaced by DMEM/FCS with or without deferoxamine (Sigma Chemical, St. Louis, MO). The culture was continued for one more day and pulse-labeled with 1.0 μCi/ml [^{3}H]thymidine during the last 6 h. The incorporated radioactivity was subjected to liquid scintillation counting, as previously described (22).

Statistical analysis. Data presented as bar graphs are the means ± SD of at least three independent experiments. Statistical analysis was performed by Student's *t*-test ($P < 0.01$ was considered significant). Kaplan-Meier survival analysis was used for survival data obtained by the log-rank test and Wilcoxon test.

Table 2. *List of primer sequences*

Genes	Forward Primers (5′-3′)	Reverse Primers (5′-3′)	TaqMan Probes (5′-3′)	Accession No.
αSMA	GAGGAGCATCCGACCTTGC	TTTCTCCCGGTTGGCCTTA	AACGGAGGCGCCGCTGAACC	NM_031004
TGFβ1	TGCTTCCGCATCACCGT	TAGTAGACGATGGGCAGTGGC	CTGCGTGCCGCAGGCTTTGG	NM_021578
PDGFRβ	ACGGCACTCAGGGTACACCT	AAGGGACCAGTTCTAGGACTCGT	ACAGGAAGCACCCACTCCTTTTAGCCC	NM_031525
IL-1β	CTTCCCCAGGACATGCTAGG	CAAAGGCTTCCCCTGGAGAC	AGCCCCCTTGTCGAGAATGGGC	NM_031512
MCP-1	CAGATGCAGTTAATGCCCCAC	AGCCGACTCATTGGGATCAT	CACCTGCTGCTACTCATTCACTGGCAA	M57441
IL-6	TGTCTCGAGCCCACCAGG	TGCGGAGAGAAACTTCATAGCTG	CGAAAGTCAACTCCATCTGCCCTTCAGG	NM_012589
TNF-α	GCTCCCTCTCATCAGTTCCATG	TACGGGCTTGTCACTCGAGTTTTG	CCCAGACCCTCACACTCAGATCATCTTC	NM_012675
COL1A2	AAGGGTCCTTCTGGAGAACC	TCGAGAGCCAGGGAGACCCA	CAGGGTCTTCTTGGTGCTCCCGGTAT	NM_053356
TIMP-2	GCCCTATGATCCCATGCTAC	TGCCCATTGATGCTCTTCTCT	CTCCCCGGATGAGTGCCTCTGGA	L31884
MMP-2	CCCCATGAAGCCTTGTTTACC	TTGTAGGAGGTGCCCTGGAA	AATGCTGATGGACAGCCCTGCA	NM_031054
GAPDH	AAGATGGTGAAGGTCGGTGTG	GAAGGCAGCCCTGGTAACC	CGGATTTGGCCGTATCGGACGC	NM_017008

αSMA, smooth muscle α-actin; TGFβ1, transforming growth factor β1; PDGFRβ, platelet-derived growth factor receptor β; MCP-1, monocyte chemotactic protein-1; COL1A2, collagen1A2; TIMP-2, tissue inhibitor of matrix metalloproteinase-2 (MMP-2).

RESULTS

Suppression of acute liver injury by an iron-deficient diet. The iron-deficient diet significantly reduced the content of iron in the liver (CD: 12.7 ± 0.6 μg/100 mg vs. ID: 1.3 ± 0.6 μg/100 mg) and the serum (CD: 175.0 ± 5.0 μg/dl vs. ID: 72.3 ± 3.7 μg/dl), as shown in Fig. 1*A*. Single-shot TAA (100 mg/body wt)-induced hepatocyte damage indicated by serum levels of AST and ALT were clearly reduced in the ID group (Fig. 1*B*). Alternatively, observation of the survival of rats with acute liver failure induced by daily TAA administration (60 mg/body wt) indicated that all CD-fed rats died within 3 days after starting TAA administration, whereas 87% of ID-fed rats survived until 4 days of TAA (Fig. 1*C*).

Decrease of hepatocyte apoptosis by iron-deficient diet. In the acute liver injury model, hepatocyte injury was observed around the central vein in the CD group (Fig. 2*A*), while lipid degeneration was observed in a few hepatocytes in the ID group (Fig. 2*B*). TUNEL-positive cells were rare in the ID group compared with the CD group (Fig. 2, *C* and *D*). Activities of both caspase-3 and -8 in liver homogenates were lower in the ID group (Fig. 2*E*).

Decrease of oxidative stress by iron-deficient diet. Acute liver injury caused oxidative DNA damage in hepatocytes, as revealed by the appearance of 8-OHdG in the nuclei (Fig. 3*A*). 8-OHdG-positive hepatocytes were abundant in the CD group, whereas they were scarce in the ID group (Fig. 3*B*). Alterna-

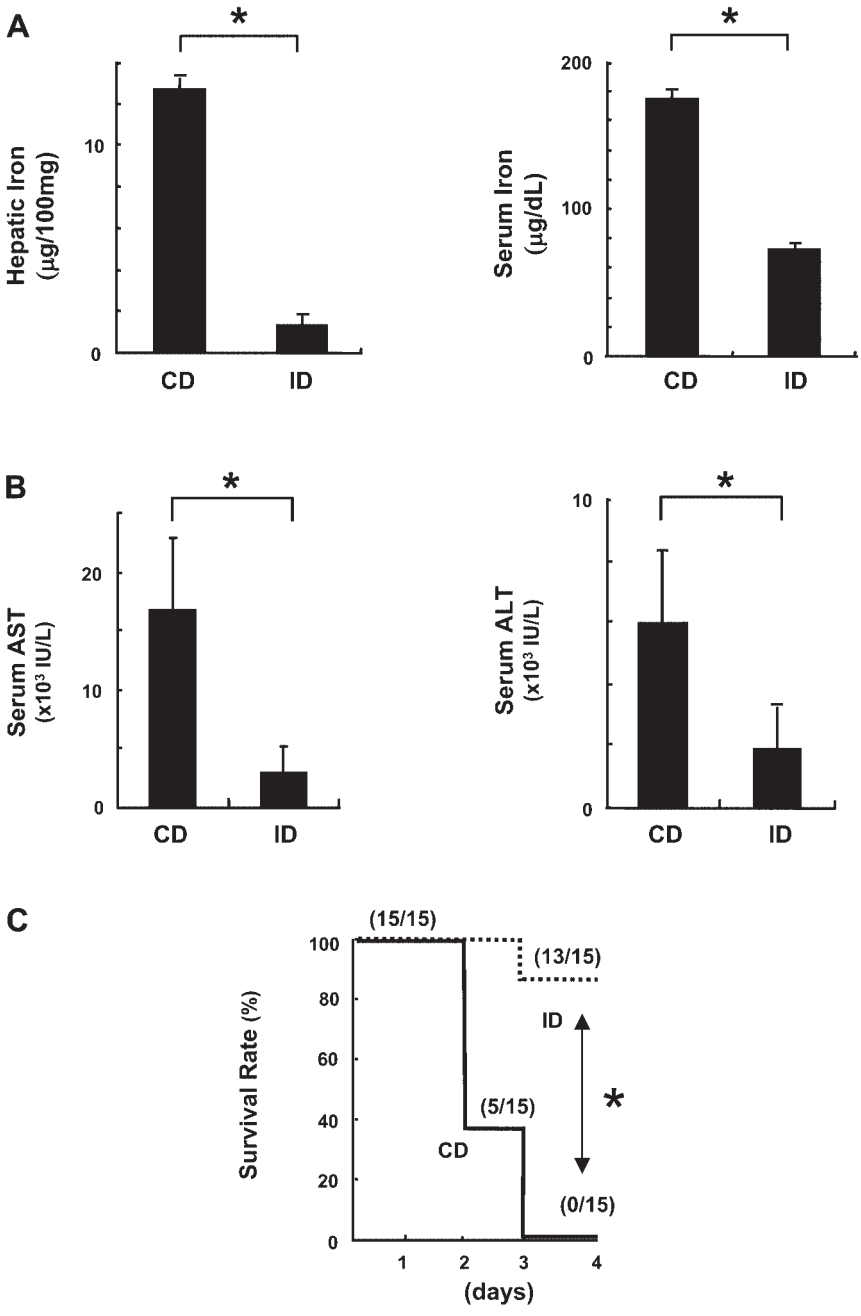

Fig. 1. Effect of iron-deficient diet on acute liver injury. *A*: free iron levels in the serum and liver. Significant differences in the levels of free iron were found in both serum and liver between the control diet (CD; $n = 5$) and the iron-deficient diet (ID; $n = 5$) rats. *$P < 0.01$. *B*: levels of aspartate aminotransferase (AST; *left*) and alanine transaminase (ALT; *right*) in serum at 48 h after thioacetamide (TAA) administration (100 mg/body). Significant differences were found in the levels of both AST and ALT between CD ($n = 5$) and ID ($n = 5$) rats. *$P < 0.01$. *C*: survival curves in the TAA-induced acute liver failure model. Rats were fed CD or ID for 4 wk. Successively, TAA (60 mg/body) was administrated to the rats every day. Survival was observed until 4 days after starting TAA administration. *$P < 0.01$.

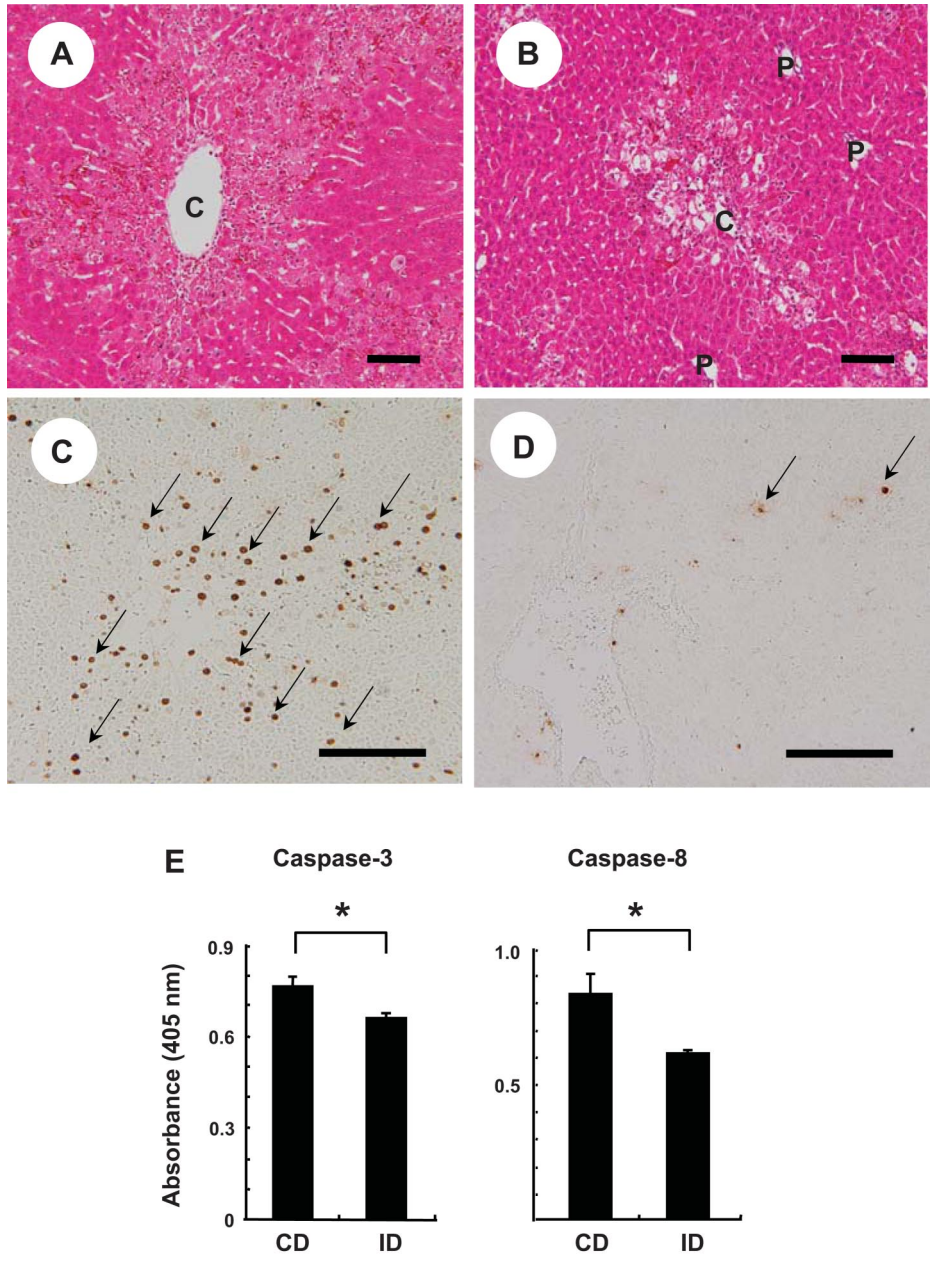

Fig. 2. Detection of apoptosis in the liver. *A*, *B*: hematoxylin and eosin (H&E) staining of the liver. *A*: CD group. *B*: ID group. Note that hepatocyte degeneration is clear in the CD group compared with the ID group. P, portal vein; C, central vein. *C*, *D*: Terminal deoxynucleotidyl transferase biotin-dUTP nick-end labeling (TUNEL) staining. *C*: CD group. *D*: ID group. Note that TUNEL-positive cells (arrows) are abundant in the CD group, whereas they are scarce in the ID group. *E*: activity of caspases in the liver. Caspase-3 and -8 activities were determined using the Caspase-3 and -8 colorimetric assay kits, respectively. Note that activity of the caspases was significantly reduced in the ID group. $*P < 0.01$. Scale bars: 100 μm.

tively, expression of 4-HNE, an a, b-unsaturated hydroxyalkene, which is produced by lipid peroxidation in cells and is one of the oxidative products, was clearly decreased in the liver homogenate of the ID group, as revealed by Western blot analysis (Fig. 3*C*). In addition, LPO, an oxidative degradation product of polyunsaturated fatty acids, was significantly reduced both in the serum and liver by ID administration (Fig. 3*D*).

Changes in mRNA expression of inflammatory and fibrogenetic genes in acute liver injury. Quantitative RT-PCR analyses revealed that the expressions of inflammatory genes such as IL-1β, monocyte chemotactic protein-1 (MCP-1), IL-6, and TNF-α were all significantly suppressed in the ID group. Expressions of mRNAs of TGF-β1, PDGFRβ, tissue inhibitor of matrix metalloproteinase-2 (TIMP-2), and matrix metalloproteinase-2 (MMP-2) were also significantly reduced in the ID group, although mRNA expressions of smooth muscle α-actin and collagen 1A2, which are markers of the activation of stellate cells, were not significantly changed (Fig. 4).

Effect of iron-deficient diet on liver fibrosis induced by TAA. Next, the effect of an iron-deficient diet on liver fibrosis induced by the repetitive injection of TAA into rats was examined. As shown in Fig. 5*A*, a macroscopic view of the liver of a CD-fed rat injected with TAA (100 mg/body wt, twice a week) for 6 wk showed a nodular surface, indicative of liver cirrhosis. In contrast, liver surfaces were smooth and nearly intact in the ID-fed group (Fig. 5*B*). Sirius Red staining of the liver revealed the development of micronodules and macronodules surrounded by collagen fibers in the CD group (Fig. 5*C*), while in the ID group, faint fibrosis was seen only around the central veins (Fig. 5*D*). Immunohistochemistry also indicated that αSMA-positive myofibroblasts were abundant in the CD group, while they were scarce in the ID group (Fig. 5,

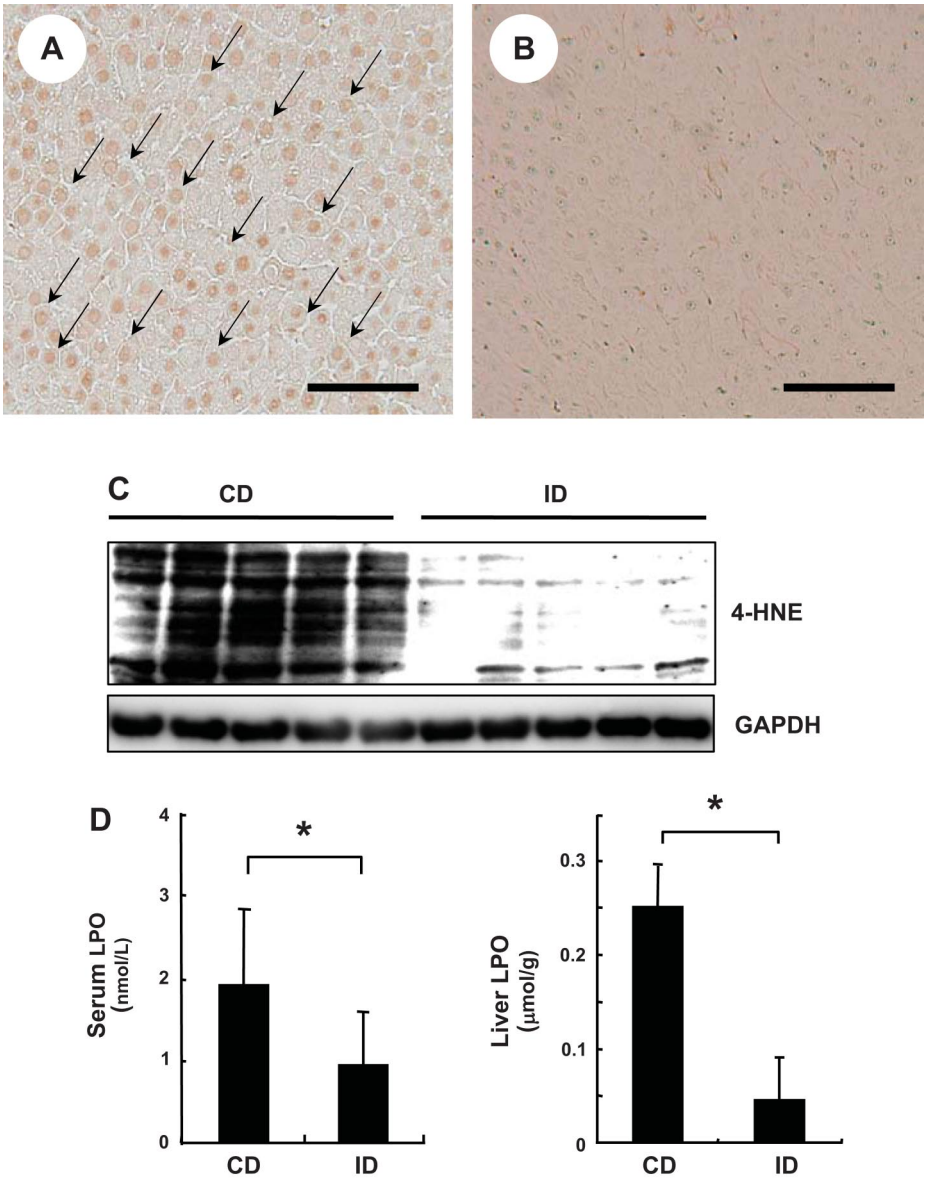

Fig. 3. Detection of oxidative stress in the liver. *A*, *B*: 8-hydroxy-2-deoxy guanosine (8-OHdG) staining of the liver. *A*: CD group. *B*: ID group. Note that 8-OHdG expression in hepatocytes is clear in the CD group (arrows) compared with the ID group. *C*: 4-Hydroxy-2-nonenal (4-HNE) expression in the liver. Liver homogenates were applied to Western blot analysis using anti-4-HNE antibodies. Note that 4-HNE was detected in proteins over a broad range of molecular weights in the CD group, while it was scarce in the ID group. *D*: serum and liver lipid peroxide (LPO) levels in the CD group and ID group. $*P < 0.01$. Scale bars: 100 μm.

E and *F*), clearly showing that the activation of stellate cells and myofibroblasts was inhibited in the ID group. At this stage, serum levels of AST and ALT were lower in the ID group than in the CD group (data not shown).

Changes in mRNA expression of inflammatory and fibrogenetic genes in chronic liver injury. Quantitative RT-PCR analyses revealed that the expressions of fibrosis-related genes such as αSMA, TGF-β1, PDGFRβ, collagen 1A2, TIMP-2, and MMP-2 were all clearly reduced in the ID group. In contrast to the acute liver injury model, expressions of MCP-1, IL-6, and TNF-α were unchanged. The expression of IL-1β mRNA was augmented in the ID group (Fig. 6).

Effect of iron-deficient diet on liver fibrosis induced by common bile duct ligation. To test whether the attenuation of liver fibrosis development by ID was reproduced in another liver fibrosis model, we used a common bile duct ligation model. In this model, hepatocyte degeneration and deposition of collagen fibers were seen in the portal vein area, whose histology sharply contrasted to the fibrosis induced by TAA (Fig. 7, *A* and *C*). As shown in Fig. 7, *B* and *D*, hepatocyte degeneration and the deposition of collagen fibers were clearly suppressed in the ID group.

Effect of deferoxamine on stellate cell activation. The results mentioned above indicate that iron may play critical roles in the occurrence of liver fibrosis, as well as acute liver injury. Recent experimental reports have revealed that hepatic stellate cells have multiple roles in the inflammatory and fibrotic responses accompanying their own activation process. Therefore, in the last series in this study, we tested the effects of deferoxamine ($C_{25}H_{48}N_6O_8$), a specific chelator of iron, otherwise known as desferrioxamine or desferal, on stellate cell function during their activation, because the removal of iron molecules from serum-containing medium is technically difficult.

As shown in Fig. 8*A*, *a*, rat stellate cells isolated and cultured for 5 days in the serum-containing medium adhered to the plastic plate and extended their cytoplasmic processes. Lipid particles, which contain vitamin A, localized around enlarged

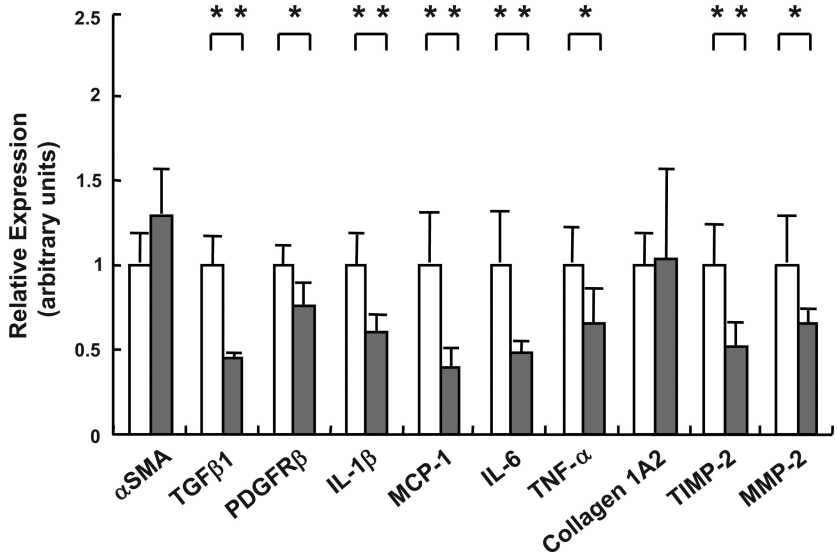

Fig. 4. Expression of inflammatory and fibrogenetic genes in the TAA-induced acute liver failure model in CD and ID groups. Total RNAs were extracted under the condition of TAA-induced acute liver failure in the CD group (white) and ID group (gray) and were subjected to real-time RT-PCR. αSMA, smooth muscle α-actin. $*P < 0.05$; $**P < 0.01$.

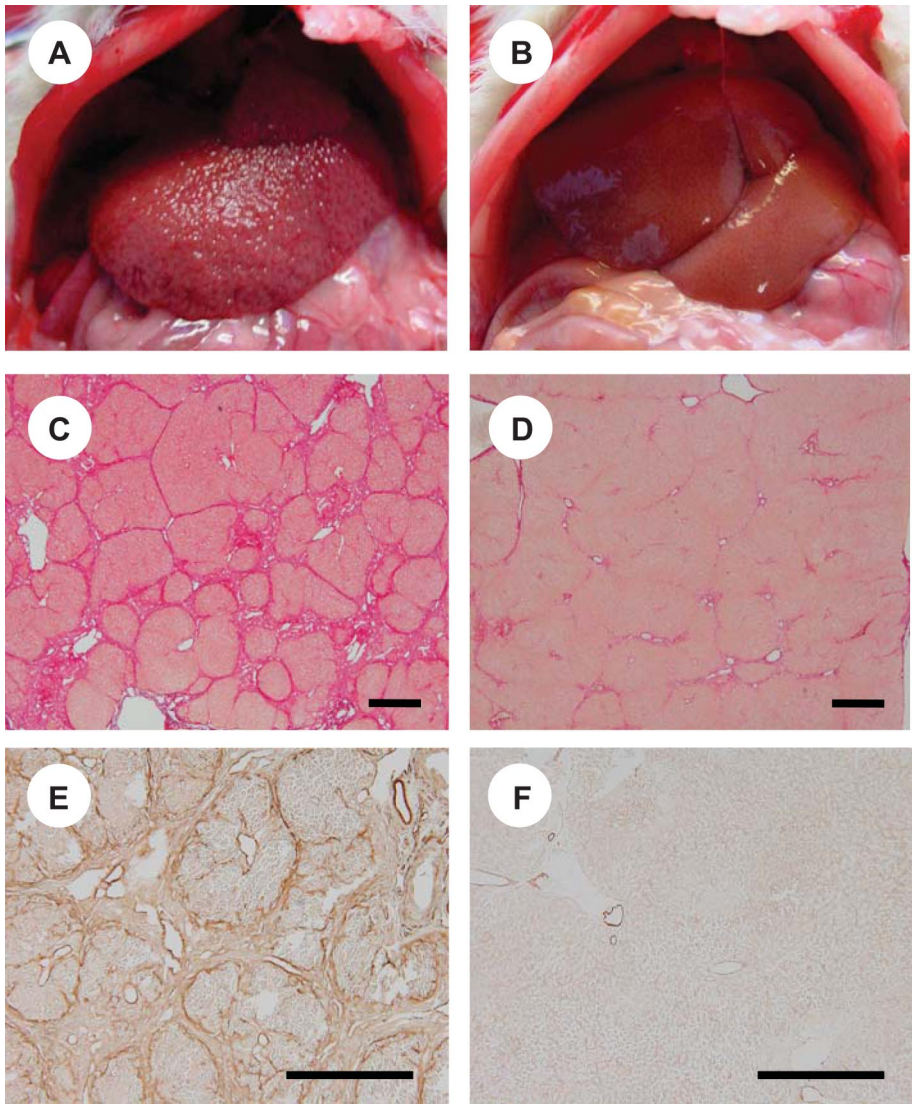

Fig. 5. Effect of an iron-deficient diet on liver fibrosis induced by TAA. *A*, *B*: macroscopic view of the liver of rats injected with TAA for 6 wk in the CD group (*left*) and ID group (*right*). *C*, *D*: Sirius Red staining in the CD group (*left*) and ID group (*right*). *E*, *F*: immunostaining of smooth muscle α-actin in the CD group (*left*) and ID group (*right*). Scale bars: 500 μm.

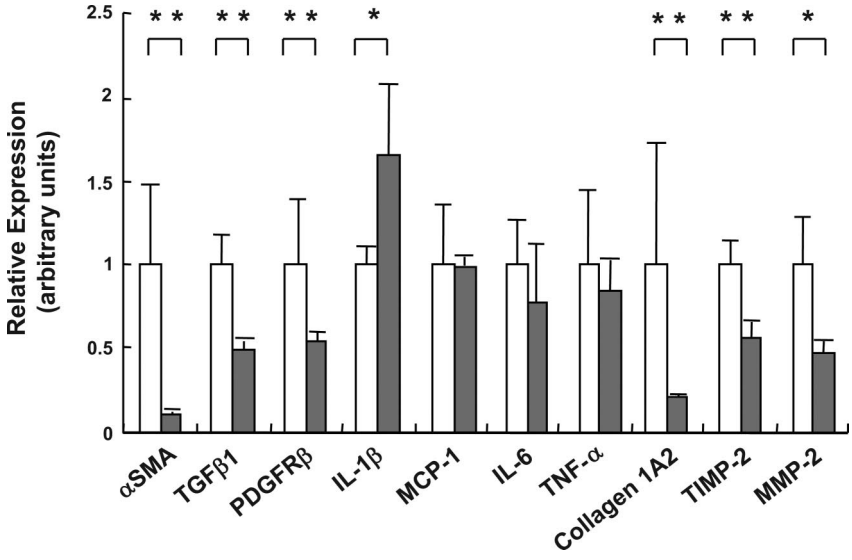

Fig. 6. Expression of inflammatory and fibrotic genes on liver fibrosis induced by TAA in CD group and ID group. Total RNAs were extracted from liver fibrosis induced by TAA in CD group (white) and ID group (gray) for real-time RT-PCR. Note that the expression of all fibrotic genes [smooth muscle α-actin (αSMA), transforming growth factor β1 (TGFβ1), platelet-derived growth factor receptor β (PDGFRβ) collagen 1A2, and tissue inhibitor of matrix metalloproteinase-2 (MMP-2) (TIMP-2)] was inhibited in the ID group. $*P < 0.05$; $**P < 0.01$.

nuclei, some of which were undergoing the process of multiplication. When they were incubated in identical medium supplemented with 10^{-4} M deferoxamine, they maintained the quiescent phenotype with dendritic processes and small nuclei (Fig. 8*A*, *b*).

The expression of markers for stellate cell activation, such as PDGFRβ and smooth muscle α-actin, was suppressed by deferoxamine in a dose-dependent manner, as revealed by Western blot analysis (Fig. 8*B*). In fact, immunofluorescence staining of αSMA confirmed the results of Western blot analysis (Fig. 8*C*).

Finally, deferoxamine inhibited [^{3}H]thymidine uptake by stellate cells in a dose-dependent manner (Fig. 8*D*), and PDGF-BB-stimulated phosphorylation of ERK and Akt (Fig. 8*E*).

DISCUSSION

The role of iron in the pathophysiology of the liver has long been studied in fields of hemochromatosis (2, 31) and alcoholic liver injury (5, 38). Recently, an unusual accumulation of iron in the liver has also been observed in chronic hepatitis C (3, 6) and nonalcoholic steatohepatitis (8, 36). Thus, research on iron homeostasis and dysregulation in the liver is one of the topics in the research field of hepatology. The upregulation and downregulation of hepcidin production by hepatocytes under pathological conditions regulates the absorption of iron from the small intestine, a process considered to represent the most important pathway (21, 23). However, medicines that regulate hepcidin production

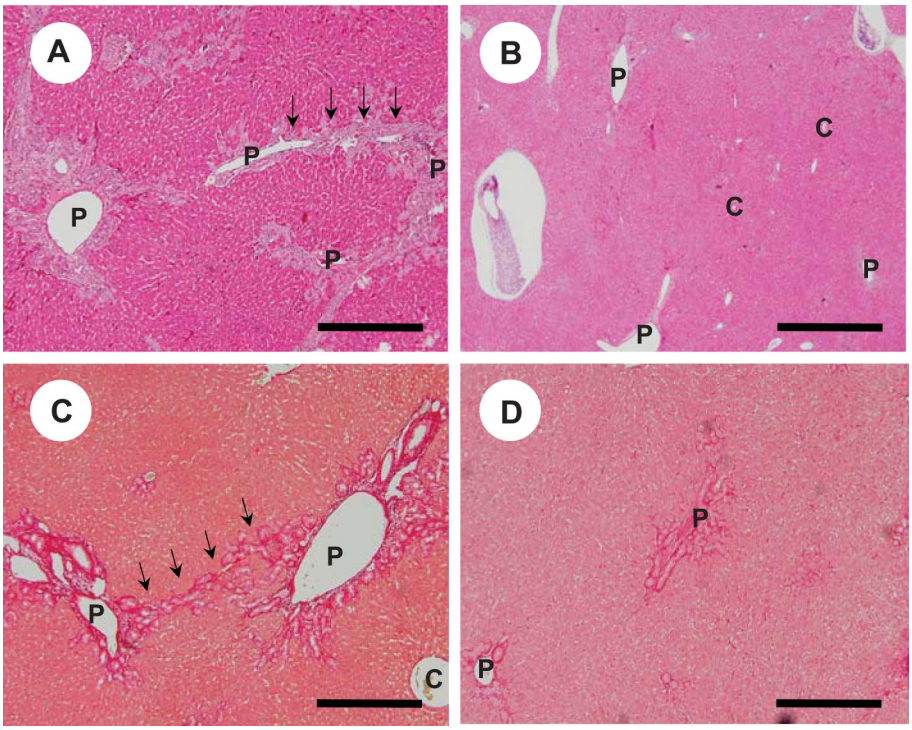

Fig. 7. Effect of iron-deficient diet on liver fibrosis induced by ligation of the common bile duct. *A*, *B*: H&E staining of the liver. *A*: CD group. *B*: ID group. Note that hepatocyte degeneration around the portal vein area is clear in the CD group compared with the ID group. P, portal vein; C, central vein. *C*, *D*: Sirius Red staining. *C*: CD group. *D*: ID group. Note that collagen deposition extended around the portal vein area in the CD group, while it was reduced in the ID group. P, portal vein; C, central vein. Arrows indicate P-P bridge formation. Scale bars: 1 mm.

have not been discovered. Phlebotomy is a relatively safe and convenient therapy to deprive iron from the body (9, 13). Body iron can be reduced by phlebotomy by 50 mg iron/100 ml. However, to maintain a low iron level, repeat phlebotomy is required, which is inconvenient for patients. In this regard, iron-chelating therapy (15, 28) and an iron-deficient diet can replace the need for phlebotomy. In particular, the clinical use of ICL670 (deferasirox), an orally administrable Fe^{3+}-chelator, in hepatic iron overload is now awaited (14, 16).

To study the effectiveness of an iron-deficient diet in the attenuation of liver injuries, we tested the effect of a low iron diet on acute and chronic liver injuries induced by TAA administration. In acute liver injury, the iron-deficient diet protected rats from liver damage and failure and improved their survival (Fig. 1). Mechanistic analyses revealed that iron depletion reduced apoptosis of hepatocytes, presumably through attenuating the activation of caspase-3 and -8 (Fig. 2). Additionally, as expected, iron depletion suppressed 8-OHdG expression in hepatocytes, as well as the expression of 4-HNE and LPO in liver tissue, indicating the role of iron in the occurrence of oxidative stress (Fig. 3). The accepted explanation for iron-induced oxidative stress is that it is caused by the Fenton pathway, which generates the hydroxyradical (·OH), a strongly reactive radical molecule (1, 7, 24, 33). This hydroxyradical modulates DNA, proteins, sugars, and biomembranes, resulting in the damage of cellular functions (4, 24, 30). Alternatively, it can be speculated that the hepatic iron increase, which probably takes place in the current TAA model, could explain protective role of iron-deficient diet. A previous report by Oliver et al. (27) indicated that the identical treatment itself resulted in increase of hepatic iron in metallothionein-I/II knockout mice. Thus, it may be speculated that iron levels will not be elevated to the same levels in iron-deficient rats compared with rats on a complete diet.

Hepatic stellate cells play pivotal roles in inflammatory and fibrotic processes in the liver (10, 32, 34). In particular, in response to oxidative stress and cytokines, including TGF-β and PDGF-BB, they change their cellular characteristics from a vitamin A-storing phenotype to matrix-producing and smooth muscle α-actin-expressing phenotypes resembling myofibroblasts present in the organs (12). The synthesis and secretion of type I collagen is upregulated, resulting in the contribution of fibrotic septum formation in the chronically inflamed liver. The activation process is triggered by oxygen free radicals, including hydrogen peroxide (H_2O_2), which can be produced by the Fenton reaction of $Fe^{2+} + H_2O_2 \rightarrow Fe^{3+} + {\cdot}HO + HO^-$. Thus, free iron may induce the activation of stellate cells, indicating that iron removal or a reduction in its content in and around stellate cells may attenuate the progression of liver fibrosis. In

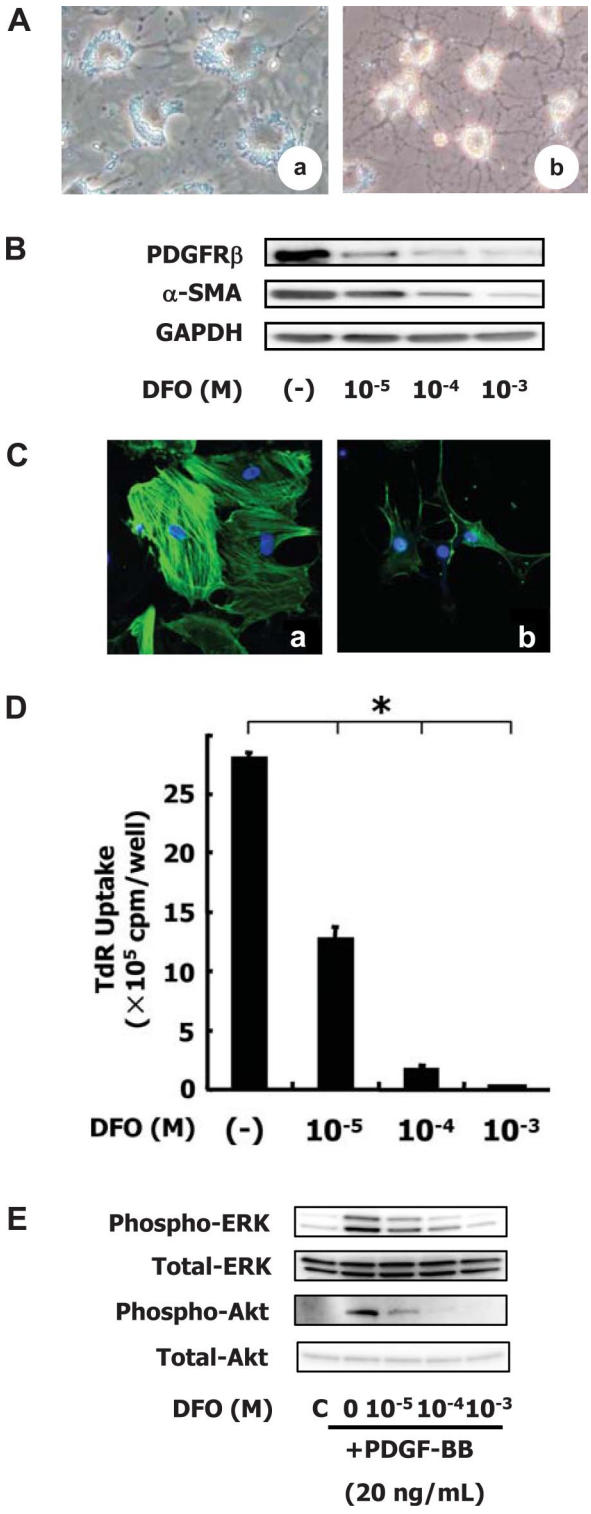

Fig. 8. Effect of deferoxamine on the activation of rat stellate cells in culture. Rat stellate cells were isolated and plated on plastic plates in serum-containing medium. At 24 h after plating, deferoxamine was added to the culture medium at the indicated concentration. *A*: morphology of stellate cells 5 days after plating. *a*: control. *b*: deferoxamine-treated cells. *B*: expression of PDGFRβ and smooth muscle α-actin in stellate cells 5 days after plating. Western blot analysis. Note that deferoxamine dose-dependently suppressed the expression of PDGFRβ and smooth muscle α-actin. DFO, deferoxamine. *C*: immunostaining of smooth muscle α-actin in stellate cells. *a*: control. *b*: deferoxamine (10^{-4} M)-treated cells. Note that stress fibers consisting of smooth muscle α-actin are well developed in nontreated control cells, while they are not organized in deferoxamine-treated cells. *D*: DNA synthesis of stellate cells. DNA synthesis was determined by the [^{3}H]thymidine incorporation assay. Note that deferoxamine suppressed DNA synthesis of stellate cells in a dose-dependent manner. *E*: effect of deferoxamine on PDGF-BB-stimulated activation of ERK and Akt pathways. Stellate cells were cultured for 5 days in the presence or absence of deferoxamine. Then, they were stimulated with PDGF-BB (20 ng/ml) for 10 min. Harvested cells were subjected to Western blot analysis to detect phospho-ERK, total ERK, phospho-Akt, and total Akt. Note that deferoxamine suppressed the phosphorylation of ERK and Akt in a dose-dependent manner.

fact, rats receiving the iron-deficient diet showed marked attenuation of the progression of liver fibrosis (Fig. 5). This is considered to have resulted from the reduction of hepatocyte damage and by the inhibition of stellate cell activation. This assumption may be supported by the results obtained using deferoxamin, showing that iron chelation inhibited the expression of PDGFRβ and αSMA, their proliferation, and PDGF-BB-dependent signal cascades such as ERK and Akt (Fig. 8).

The role of Kupffer cells in the attenuation of liver damage by an iron-deficient diet should also be considered. Iron has been reported as a critical factor for the regulation of Kupffer cell activation with respect to alcoholic liver disease (35, 39). Ionic iron (Fe^{2+}) is reported to activate NF-κB, resulting in the enhanced production of TNF-α (35, 39). In this study, we observed the reduction of mRNA expression via iron-deficient diet administration of IL-1β, MCP-1, IL-6, and TNF-α, all of which are NF-κB-dependent genes (Fig. 4). Although we did not determine the free iron content in Kupffer cells, reduction of the iron content in the liver hampers NF-κB and inflammatory gene expression.

Perspectives and Significance

An iron-deficient diet is effective in reducing hepatocyte damage in the acute liver injury model and in the attenuation of liver fibrosis in the chronic model. Attenuation of hepatocyte apoptosis is considered to be caused by the reduction of oxidative stress and decrease of inflammatory gene expression. Furthermore, iron is speculated to be a key molecule in the progression of stellate cell activation and ECM gene expression. The control of iron homeostasis in the liver can be a therapeutic strategy for chronic liver disorder.

ACKNOWLEDGMENTS

The authors thank to Ms. Michiko Ohashi for her technical assistance. This study was supported by a Grant-In-Aid for Scientific Research from the Japan Society for the Promotion of Science (to N. Kawada).

REFERENCES

1. **Aisen P, Enns C, and Wessling-Resnick M.** Chemistry and biology of eukaryotic iron metabolism. *Int J Biochem Cell Biol* 33: 940–959, 2001.
2. **Beutler E, Hoffbrand AV, Cook JD.** Iron deficiency and overload. *Hematology Am Soc Hematol Educ Program* 40–61, 2003.
3. **Bonkovsky HL, Banner BF, Rothman AL.** Iron and chronic viral hepatitis. *Hepatology* 25: 759–768, 1997.
4. **Caro AA, Cederbaum AI.** Oxidative stress, toxicology, and pharmacology of CYP2E1. *Annu Rev Pharmacol Toxicol* 44: 27–42, 2004.
5. **Dey A, Cederbaum AI.** Alcohol and oxidative liver injury. *Hepatology* 43: S63-S74, 2006.
6. **Di Bisceglie AM, Axiotis CA, Hoofnagle JH, Bacon BR.** Measurements of iron status in patients with chronic hepatitis. *Gastroenterology* 102: 2108–2113, 1992.
7. **Eisenstein RS.** Iron regulatory proteins and the molecular control of mammalian iron metabolism. *Annu Rev Nutr* 20: 627–662, 2000.
8. **Fargion S, Mattioli M, Fracanzani AL, Sampietro M, Tavazzi D, Fociani P, Taioli E, Valenti L, Fiorelli G.** Hyperferritinemia, iron overload, and multiple metabolic alterations identify patients at risk for nonalcoholic steatohepatitis. *Am J Gastroenterol* 96: 2448–2455, 2001.
9. **Fontana RJ, Israel J, LeClair P, Banner BF, Tortorelli K, Grace N, Levine RA, Fiarman G, Thiim M, Tavill AS, Bonkovsky HL.** Iron reduction before and during interferon therapy of chronic hepatitis C: results of a multicenter, randomized, controlled trial. *Hepatology* 31: 730–736, 2000.
10. **Friedman SL.** Seminars in medicine of the Beth Israel Hospital, Boston. The cellular basis of hepatic fibrosis Mechanisms and treatment strategies. *N Engl J Med* 328: 1828–1835, 1993.
11. **Fujita N, Horiike S, Sugimoto R, Tanaka H, Iwasa M, Kobayashi Y, Hasegawa K, Ma N, Kawanishi S, Adachi Y, Kaito M.** Hepatic oxidative DNA damage correlates with iron overload in chronic hepatitis C patients. *Free Radic Biol Med* 42: 353–362, 2007.
12. **Galli A, Svegliati-Baroni G, Ceni E, Milani S, Ridolfi F, Salzano R, Tarocchi M, Grappone C, Pellegrini G, Benedetti A, Surrenti C, Casini A.** Oxidative stress stimulates proliferation and invasiveness of hepatic stellate cells via a MMP2-mediated mechanism. *Hepatology* 41: 1074–1084, 2005.
13. **Hayashi H, Takikawa T, Nishimura N, Yano M, Isomura T, Sakamoto N.** Improvement of serum aminotransferase levels after phlebotomy in patients with chronic active hepatitis C and excess hepatic iron. *Am J Gastroenterol* 89: 986–988, 1994.
14. **Hershko C, Konijn AM, Nick HP, Breuer W, Cabantchik ZI, Link G.** ICL670A: a new synthetic oral chelator: evaluation in hypertransfused rats with selective radioiron probes of hepatocellular and reticuloendothelial iron stores and in iron-loaded rat heart cells in culture. *Blood* 97: 1115–1122, 2001.
15. **Hoffbrand AV, Gorman A, Laulicht M, Garidi M, Economidou J, Georgipoulou P, Hussain MA, Flynn DM.** Improvement in iron status and liver function in patients with transfusional iron overload with long-term subcutaneous desferrioxamine. *Lancet* 1: 947–949, 1979.
16. **Ibrahim AS, Gebermariam T, Fu Y, Lin L, Husseiny MI, French SW, Schwartz J, Skory CD, Edwards JE, Spellberg BJ.** The iron chelator deferasirox protects mice from mucormycosis through iron starvation. *J Clin Invest* 117: 2649–2657, 2007.
17. **Ishizaka N, Saito K, Noiri E, Sata M, Ikeda H, Ohno A, Ando J, Mori I, Ohno M, Nagai R.** Administration of ANG II induces iron deposition and upregulation of TGF-beta1 mRNA in the rat liver. *Am J Physiol Regul Integr Comp Physiol* 288: R1063–R1070, 2005.
18. **Kato J, Kobune M, Nakamura T, Kuroiwa G, Takada K, Takimoto R, Sato Y, Fujikawa K, Takahashi M, Takayama T, Ikeda T, Niitsu Y.** Normalization of elevated hepatic 8-hydroxy-2′-deoxyguanosine levels in chronic hepatitis C patients by phlebotomy and low iron diet. *Cancer Res* 61: 8697–8702, 2001.
19. **Kinoshita K, Iimuro Y, Otogawa K, Saika S, Inagaki Y, Nakajima Y, Kawada N, Fujimoto J, Friedman SL, Ikeda K.** Adenovirus-mediated expression of BMP-7 suppresses the development of liver fibrosis in rats. *Gut* 56: 706–714, 2007.
20. **Kristensen DB, Kawada N, Imamura K, Miyamoto Y, Tateno C, Seki S, Kuroki T, Yoshizato K.** Proteome analysis of rat hepatic stellate cells. *Hepatology* 32: 268–277, 2000.
21. **Lee P, Peng H, Gelbart T, Wang L, Beutler E.** Regulation of hepcidin transcription by interleukin-1 and interleukin-6. *Proc Natl Acad Sci USA* 102: 1906–1910, 2005.
22. **Maeda N, Kawada N, Seki S, Arakawa T, Ikeda K, Iwao H, Okuyama H, Hirabayashi J, Kasai K, Yoshizato K.** Stimulation of proliferation of rat hepatic stellate cells by galectin-1 and galectin-3 through different intracellular signaling pathways. *J Biol Chem* 278: 18938–18944, 2003.
23. **Nicolas G, Chauvet C, Viatte L, Danan JL, Bigard X, Devaux I, Beaumont C, Kahn A, Vaulont S.** The gene encoding the iron regulatory peptide hepcidin is regulated by anemia, hypoxia, and inflammation. *J Clin Invest* 110: 1037–1044, 2002.
24. **Okada S.** Iron-induced tissue damage and cancer: the role of reactive oxygen species-free radicals. *Pathol Int* 46: 311–332, 1996.
25. **Okuyama H, Nakamura H, Shimahara Y, Araya S, Kawada N, Yamaoka Y, Yodoi J.** Overexpression of thioredoxin prevents acute hepatitis caused by thioacetamide or lipopolysaccharide in mice. *Hepatology* 37: 1015–1025, 2003.
26. **Okuyama H, Shimahara Y, Kawada N, Seki S, Kristensen DB, Yoshizato K, Uyama N, Yamaoka Y.** Regulation of cell growth by redox-mediated extracellular proteolysis of platelet-derived growth factor receptor beta. *J Biol Chem* 276: 28274–28280, 2001.
27. **Oliver JR, Jiang S, Cherian MG.** Augmented hepatic injury followed by impaired regeneration in metallothionein-I/II knockout mice after treatment with thioacetamide. *Toxicol Appl Pharmacol* 210:190–199, 2006.
28. **Olivieri NF, Brittenham GM, McLaren CE, Templeton DM, Cameron RG, McClelland RA, Burt AD, Fleming KA.** Long-term safety and effectiveness of iron-chelation therapy with deferiprone for thalassemia major. *N Engl J Med* 339: 417–423, 1998.
29. **Otogawa K, Kinoshita K, Fujii H, Sakabe M, Shiga R, Nakatani K, Ikeda K, Nakajima Y, Ikura Y, Ueda M, Arakawa T, Hato F, Kawada N.** Erythrophagocytosis by liver macrophages (Kupffer cells) promotes oxidative stress, inflammation, and fibrosis in a rabbit model of steatohepatitis: implications for the pathogenesis of human nonalcoholic steatohepatitis. *Am J Pathol* 170: 967–980, 2007.

30. **Papanikolaou G, Pantopoulos K.** Iron metabolism and toxicity. *Toxicol Appl Pharmacol* 202: 199–211, 2005.
31. **Pietrangelo A.** Hereditary hemochromatosis-a new look at an old disease. *N Engl J Med* 350: 2383–2397, 2004.
32. **Pinzani M, Marra F.** Cytokine receptors and signaling in hepatic stellate cells. *Semin Liver Dis* 21: 397–416, 2001.
33. **Ponka P.** Tissue-specific regulation of iron metabolism and heme synthesis: distinct control mechanisms in erythroid cells. *Blood* 89: 1–25, 1997.
34. **Ramm GA, Ruddell RG.** Hepatotoxicity of iron overload: mechanisms of iron-induced hepatic fibrogenesis. *Semin Liver Dis* 25: 433–449, 2005.
35. **She H, Xiong S, Lin M, Zandi E, Giulivi C, Tsukamoto H.** Iron activates NF-κB in Kupffer cells. *Am J Physiol Gastrointest Liver Physiol* 283: G719–G726, 2002.
36. **Sumida Y, Nakashima T, Yoh T, Furutani M, Hirohama A, Kakisaka Y, Nakajima Y, Ishikawa H, Mitsuyoshi H, Okanoue T, Kashima K, Nakamura H, Yodoi J.** Serum thioredoxin levels as a predictor of steatohepatitis in patients with nonalcoholic fatty liver disease. *J Hepatol* 38: 32–38, 2003.
37. **Toyokuni S, Sagripanti JL.** Association between 8-hydroxy-2′-deoxyguanosine formation and DNA strand breaks mediated by copper and iron. *Free Radic Biol Med* 20: 859–864, 1996.
38. **Tsukamoto H, Horne W, Kamimura S, Niemela O, Parkkila S, Yla-Herttuala S, Brittenham GM.** Experimental liver cirrhosis induced by alcohol and iron. *J Clin Invest* 96: 620–630, 1995.
39. **Tsukamoto H, Lin M, Ohata M, Giulivi C, French SW, Brittenham G.** Iron primes hepatic macrophages for NF-κB activation in alcoholic liver injury. *Am J Physiol Gastrointest Liver Physiol* 277: G1240–G1250, 1999.